

STRUCTURAL AND THERMAL BEHAVIOR OF COAL COMBUSTION AND GASIFICATION BY-PRODUCTS: SEM, FTIR, DSC, and DTA Measurements

P. S. Valimbe¹, V. M. Malhotra¹, and D. D. Banerjee².

1. Department of Physics, Southern Illinois University, Carbondale, Illinois 62901-4401

2. Illinois Clean Coal Institute, Carterville, Illinois 62918-0008.

Keywords: Coal combustion residues, scrubber sludge, thermal and spectroscopic characterization

ABSTRACT

The pulverized coal combustion fly ash, fluidized bed combustion fly ash, fluidized bed combustion spent bed ash, and scrubber sludge samples were systematically characterized using scanning electron microscopy (SEM), differential scanning calorimetry (DSC), differential thermal analysis (DTA), and transmission Fourier transform infrared (FTIR) techniques. Our spectroscopic results indicated that the scrubber sludge is mainly composed of a gypsum-like phase whose lattice structure does not exactly match either conventional gypsum ($\text{CaSO}_4 \cdot 2\text{H}_2\text{O}$) or hanebachite ($\text{CaSO}_3 \cdot 0.5\text{H}_2\text{O}$). SEM images suggested that unlike PCC fly ash particles, which were mainly spherical, the FBC fly ash and FBC spent bed ash particles were irregularly shaped and showed considerable fusion. FBC fly ashes were mainly composed of anhydrite, lime, portlandite, calcite, hematite, magnetite, and various glass phases. The DTA and DSC data presented evidence implying that the PCC fly ash is thermally stable at $30^\circ\text{C} < T < 1100^\circ\text{C}$. However, this was not the case for FBC ashes.

INTRODUCTION

More than 800 million tons of coal per year are burned in the United States, producing approximately 10 % of the coal burned as combustion residues in the form of solids. These solids, which are largely noncombustible, are classified as "fly ash" and "bottom ash". The fly ash particles are fine materials which are mostly captured in precipitators and in bag houses. The bottom ash term is used for those materials which settle or flow as melt to the bottom of the boiler. If the boiler is designed to use pulverized coal, then the coal combustion by-products are called "pulverized coal combustion" (PCC) fly ash and PCC bottom ash.

The midwestern USA coals are high in sulfur content. The sulfur in coal is in the form of inorganic minerals (chiefly pyrite) and is also organically bound. Therefore, environmental concerns require that the sulfur content of the coal be reduced if this abundant resource is to be continuously utilized. A two prong approach is being developed to mitigate the sulfur problem. In the first, physical, chemical, and microbiological coal cleaning techniques have been and are being developed to reduce the sulfur content of midwestern coals. In the second, technologies have been developed and are being perfected to capture sulfur-containing combustion gases during coal combustion. One such clean coal technology is fluidized bed combustion (FBC)^{1,2}. The advantage of the FBC technology is that it affords a large reduction of SO_2 from the combustion gases. The sorbents, like calcium carbonate (CaCO_3) and calcium oxide (CaO), are injected along with the coal into FBC combustor. As SO_2 is produced, it reacts with the sorbent and is captured in the form of anhydrous calcium sulfate (CaSO_4)^{1,3}. There are also reports in the literature which suggest the formation of sulfides⁴. Just like for conventional combustors, two types of solid residues are produced, e.g., FBC fly ash, which leaves the combustor at the top, and FBC spent bed ash, which is left at the bottom of the combustor.

Wet scrubber processes are extensively used in flue gas desulfurization (FGD) technology. The major waste products produced are gypsum, calcium sulfite (CaSO_3), fly ash, and excess reagents⁵. Calcium sulfite may be oxidized to calcium sulfate which in combination with water forms gypsum. It is generally believed that the calcium sulfate purity of residues from wet scrubber technology using lime or limestone ranges between 95 % to 99 %.

It is estimated that by the turn of century about 200 million tons of coal combustion residue will be produced annually. With the current cost of residue disposal expected to rapidly escalate, the economic stakes for the coal utilization industry are substantial. Consequently, the technologies which can convert combustion residues into high value, but economically sound, materials are of utmost importance. Presently, only about 25% of the combustion residues generated are utilized⁶, with the rest going to landfill or surface impoundments. Therefore, efforts are underway to find alternative usage^{6,9} of the combustion residues, e.g., ultra-lightweight aggregates for insulation industry, Portland cement-based FBC mixes, highway and street construction, construction bricks or tiles, roofing or paving tiles, pipe construction, and ashalloys. We have recently initiated research in our laboratory in which we are attempting to form advanced composite materials from coal combustion residues obtained from Illinois utilities. However, the successful utilization of coal

combustion and gasification residues requires a thorough physical and chemical characterization of these ashes.

EXPERIMENTAL TECHNIQUES

For our characterization studies, we examined four samples, i.e., PCC fly ash (Baldwin), FBC fly ash (ADM), FBC spent bed ash (ADM), and scrubber sludge (CWLP). The residue samples were obtained from the sample bank established at the Mining Engineering Department of Southern Illinois University at Carbondale. The magnetic content of PCC fly ash, FBC fly ash, and FBC spent bed ash was extracted from the as-received ashes by applying a magnetic separation technique.

Microscopic studies of the coal combustion residues were accomplished using a Hitachi S570 scanning electron microscope. The samples were mounted on the SEM sample stubs using sticky tabs. The mounted samples were then cured at 60°C for 24 hours to ensure that the ash particles would not detach from the stub while under the electron beam. After curing, the samples were sputter coated with 40 nm of gold layer to help eliminate the problem of sample charging. The SEM data were collected using an accelerating voltage of 20 kV, except for FBC spent bed ash whose SEM pictures were acquired at an accelerating voltage of 10 kV to reduce sample charging.

The structural characteristics of the combustion ashes and scrubber sludge were probed by recording their FTIR spectra. We used KBr pellet technique to collect the infrared spectra on a IBM IR44 FTIR spectrometer. One hundred scans were acquired at a 4 cm⁻¹ resolution. Since the as-received scrubber sludge sample was wet, i.e., had substantial amount of moisture in it, the sludge was dried at 100°C prior to making its KBr pellets.

The thermal behavior of coal combustion residues and scrubber sludge were obtained using DSC and DTA techniques. The DSC data were recorded on PCC fly ash, FBC fly ash, FBC spent bed ash, and scrubber sludge using a well calibrated¹⁰⁻¹² Perkin-Elmer DSC7 system interfaced with a 486 PC computer. The procedures adopted for the calibration of the temperature and of the specific heat have been described elsewhere¹². Our calibrated DSC system had a temperature precision of ± 1 K. The thermal characteristics of the residues using DSC technique were ascertained at 30°C < T < 600°C. We used a heating rate of 20°C/min under a controlled N₂ purge environment (30 cm³/min) to collect our DSC data.

The thermal stability of fly ashes, spent bed ash and scrubber sludge at 50°C < T < 1010° was examined by acquiring DTA data using a Perkin-Elmer DTA7 system. The samples were heated from 50°C to 1000°C under a nitrogen gas environment. The heating rate used was 20°C/min.

RESULTS AND DISCUSSION

Microscopic Studies: Figures 1, 2, 3, and 4 reproduce the SEM micrographs of PCC fly ash, FBC fly ash, FBC spent bed ash, and scrubber sludge, respectively. The PCC fly ash particles were mainly composed of spherically-shaped particles whose sizes ranged from 0.2 mm to 15 mm. The spherical particles were usually hollow. It should be noted from Fig. 1 that small spherical particles of PCC fly ash were attached to bigger fly ash particles giving the appearance of agglomerates. Our SEM data on PCC fly ash did show some irregularly shaped particles in the ash, but predominantly particles were spherical. From the SEM micrographs of FBC fly ash, it appears that this ash had small particles of the range 0.1 mm to 1 mm, which had fused together to form agglomerates of the size ranging from 2 mm to 100 mm. Our SEM micrographs also indicated that the FBC fly ash contained very little spherical particles unlike PCC fly ash. The lack of the presence of spherical particles in FBC fly ash may be due to the lower combustion temperatures¹⁻² for FBC combustor (around 850°C) than for PCC combustor (around 1150°C). The microscopic analysis of the FBC spent bed ash exhibited three distinct types of particles in this ash material. The first type of particles had a smooth surface to which smaller particles (i.e., 2 mm - 10 mm) were fused. These smooth particles lacked any pore structure. The second type of particles showed varying shapes and sizes but generally was around 750 mm. The third type of particles in this ash had a glass-like structure. These particles had an extensive pore structure, as can be seen in Fig. 3, and their sizes ranged from 250 mm - 300 mm. Figure 4 reproduces the SEM micrographs of scrubber sludge particles which were dried at room temperature. Generally, the sludge particles had a whisker-like shape, ranging from 50 mm to 400 mm in length, and were about 50 mm thick. In addition to the whisker-like particles, the sludge had some agglomerated particles whose average size was about 100 mm.

Thermal Behavior: The thermal stability of the PCC fly ash, FBC fly ash, FBC spent bed ash, and scrubber sludge was probed by recording their DSC and DTA data. The main thermal events observed from our DSC results are summarized in Table 1. The high temperature thermal stability of the combustion residues was ascertained by collecting DTA data at 50°C - 1000°C. We summarize our DTA results in Table 2, and Fig. 5 depicts typical DTA curves obtained from the combustion residues and scrubber sludge. The thermal data can be summarized as follows: (a) The PCC fly ash

contained moisture which was evolved on heating the ash at 155°C and 185°C. Besides these two minor endothermic reactions, the DTA curve of PCC fly ash depicted an additional weak endothermic peak at 574°C. It is well known¹³ that β -quartz undergoes transformation to α -quartz at 573°C. Therefore, the weak endotherm observed at 574°C for the PCC fly ash could be assigned to the presence of quartz in the ash. Our PCC fly ash sample, besides minor endothermic reactions at 155, 185, and 574°C, remained thermally inert up to 1000°C, thus making it an excellent raw material for the fabrication of composite materials. (b) It should be noted from Tables 1 and 2 that the FBC fly ash and FBC spent bed ash appeared to have similar thermal behaviors, i.e., thermal decomposition reaction at ~438°C which could be associated with the decomposition¹⁴ of $\text{Ca}(\text{OH})_2$ into CaO and H_2O . The presence of $\text{Ca}(\text{OH})_2$ in the FBC fly ash and FBC spent bed ash was not entirely surprising notwithstanding that these ashes were subjected to combustion temperatures of around 850°C. The probable source of $\text{Ca}(\text{OH})_2$ in our ashes could be moisture's reaction with CaO during the storage of ash material.

TABLE 1
Summary of the Thermal Events of the Combustion Residues as Determined by DSC at
30°C < T < 590°C.

Sample	Thermal Event	Temperature (°C)	% Weight Loss on Heating the sample to 580°C
PCC Fly Ash	-	-	4.4
FBC Fly Ash	Endothermic	420	2.7
FBC Spent Bed Ash	Endothermic	420	1
Scrubber Sludge	Endothermic	141	17.2
	Endothermic	176	
	Exothermic	380	

The additional endothermic event at 674°C for FBC fly ash strongly suggested the presence of hematite ($\alpha\text{-Fe}_2\text{O}_3$) in this ash. It should be noted from Fig. 5 that this thermal event was absent from the spent bed ash's DTA curve. The weak endothermic peak could be assigned to the magnetic transformation of hematite¹³. (c) The DSC and DTA curves for the scrubber sludge showed a strong endothermic peak at 180°C and a weak exothermic peak at 380°C. The endothermic peak at 180°C suggested the dehydration of the gypsum, i.e.,



From their thermogravimetric experiments, Dorsey and Buecker¹⁵ suggested the presence of calcium sulfite in their sample of scrubber sludge. They reported weight loss at 408°C < T < 452°C from their sample and associated this weight loss with the dehydration of hemihydrate ($\text{CaSO}_3 \cdot \text{CaSO}_4 \cdot 1/2\text{H}_2\text{O}$), i.e.,



As listed in Table 2, the exothermic peak at 380°C for our scrubber sludge sample began at around 348°C and terminated at around 493°C. Therefore, one may argue that the exothermic peak at 380°C could be assigned to the dehydration of hemihydrate. The FTIR spectrum of our scrubber sludge sample did not show any oscillators at 970 and 945 cm^{-1} due to sulfite ions. Moreover, dehydration should produce an endothermic peak. It has been reported in the literature¹⁶ that on heating gypsum it undergoes a polymorphous transformation at 370°C < T < 460°C which results in a weak, exothermic peak. Therefore, we assigned the exothermic peak at 380°C for our scrubber sludge to this polymorphous transition.

Spectroscopic Characterization: The spectroscopic studies of various combustion residues were undertaken to characterize the mineral and glass phases of the PCC fly ash, FBC fly ash, FBC spent bed ash, and scrubber sludge. In Fig. 7 we have reproduced the transmission-FTIR spectrum of scrubber sludge particles which were air dried prior to recording their spectrum. Three very strong bands were observed at 1154, 1126, and 1105 cm^{-1} . In addition, a doublet having frequencies 662 and 602 cm^{-1} was observed. In the water's stretching region, two distinct vibrational modes could be seen at 3617 and 3559 cm^{-1} . In the water's bending region only a single oscillator was observed at

1620 cm^{-1} . It is generally believed that the FGD residue, e.g., scrubber sludge, contains calcite (CaCO_3), hannebachite ($\text{CaSO}_4 \cdot 0.5\text{H}_2\text{O}$), gypsum ($\text{CaSO}_4 \cdot 2\text{H}_2\text{O}$), quartz (SiO_2), and troilite (FeS). The absence of any vibrational bands below 450 cm^{-1} led us to discount the presence of troilite in our sample. Since we did not observe any band in the FTIR spectrum of the scrubber sludge at around 1430 cm^{-1} , we could also rule out the presence of calcite particles in our sludge sample. The argument that quartz may be present in our sample was discarded because the diagnostic bands for it at around 1050 and 472 cm^{-1} were not observed in our FTIR spectrum. However, our transmission-FTIR data did suggest the presence of gypsum. The vibrational bands at 1154, 1126, and 1105 cm^{-1} could be assigned to ν_3 of sulfate of gypsum, while the oscillators at 662 and 602 cm^{-1} could be attributed to ν_4 of sulfate ions. The presence of two vibrational modes in the water's stretching region implied that there are two types of hydrates in our scrubber sludge. A comparison of a commercially available gypsum's FTIR spectrum, see Fig. 7, with our scrubber sludge spectrum indicated that gypsum formed in the FGD residue had a lattice structure which was different from that of commercial gypsum. It is worth pointing out that the FTIR spectrum of bassanite ($\text{CaSO}_4 \cdot 0.5\text{H}_2\text{O}$) shows a vibrational mode at about 3615 cm^{-1} and we observed a band at 3617 cm^{-1} . However, we could not assign 3617 cm^{-1} band to bassanite because the accompanying water band at 3465 cm^{-1} was absent in our spectrum. We also ruled out the presence of hannebachite because of two reasons, i.e., (a) we did not observe the expected strong bands at 975 and 940 cm^{-1} of SO_4 ion in our FTIR spectrum of the scrubber sludge, and (b) we did not see any rectangular crystals, which could be associated with hannebachite, in our SEM images of the sludge. In

TABLE 2
The Thermal Characteristics of the Combustion Residues as determined by DTA
at $50^\circ\text{C} < T < 1100^\circ\text{C}$.

Sample	Peak Begins ($^\circ\text{C}$)	Peak Ends ($^\circ\text{C}$)	Peak Temperature ($^\circ\text{C}$)
PCC Fly Ash			155
	460	701	185
			574
FBC Fly Ash	348	542	438
	615	729	674
FBC Spent Bed Ash	190	245	205
	344	491	442
Scrubber Sludge	96	275	180
	348	493	380

view of the discussion presented above we argue that scrubber sludge is mainly composed of gypsum. However, its lattice structure is not identical to the lattice structure of conventional gypsum.

The transmission-FTIR spectrum of PCC fly ash, FBC fly ash, and FBC spent bed ash is reproduced in Fig. 7, and the observed frequencies are listed in Table 3. Based on the observed FTIR spectrum, it is argued that PCC fly ash is largely composed of various oxides. The strongest bands in our transmission-FTIR spectrum of PCC fly ash originated from quartz. The transmission-FTIR spectrum of as-received FBC fly suggested the presence of quartz, anhydrite (CaSO_4), lime (CaO), portlandite ($\text{Ca}(\text{OH})_2$), calcite, hematite (Fe_2O_3), magnetite (Fe_3O_4), and glass phases. From the observed infrared frequencies of FBC spent bed ash, which are listed in Table 3, the following minerals have been identified, i.e., anhydrite, lime, portlandite, calcite, periclase, hematite, and magnetite. It is also generally reported that spent bed ash contains CaS. The formation of CaS is believed to occur for circulating fluidized bed combustion (FBC) via the following reaction, i.e., $\text{CaO} + \text{H}_2\text{S} \rightarrow \text{CaS} + \text{H}_2\text{O}$. However, it is difficult for us to confirm the presence of CaS in our FBC spent bed ash as CaS produces no infrared bands.

ACKNOWLEDGMENTS

This research was supported by grants made possible by the U. S. Department of Energy Cooperative Agreement Number DE-FC22-92PC92521 and the Illinois Department of Energy through the Illinois Coal Development Board and the Illinois Clean Coal Institute. Neither the authors nor the U. S. Department of Energy, Illinois Clean Coal Institute, nor any person acting on behalf of either: (A) Make any warranty of representation, express or implied, with respect to the accuracy, completeness, or usefulness of the information contained in this report, or that the use of

any information, apparatus, method, or process disclosed in this report may not infringe privately-owned rights; or (B) Assume any liabilities with respect to the use of, or for damages resulting from the use of, any information, apparatus, method or process disclosed in this report. References herein to any specific commercial product, process, or service by trade name, trademark, manufacturer, or otherwise, does not necessarily constitute or imply its endorsement, recommendation, or favoring by the U. S. Department of Energy. The views and opinions of authors expressed herein do not necessarily state or reflect those of the U. S. Department of Energy.

REFERENCES

1. M. Valk, "Fluidized Bed Combustors" in 'Fluidized Bed Combustion', M. Radovanovic, Ed., Hemisphere Publishing Co., Washington (1986).
2. L. Yaverbaum, 'Fluidized Bed Combustion of Coal and Waste Materials', Noyes Data Co. (1977).
3. R. J. Collins, J. Testing and Evaluation **8**, 259 (1980).
4. E. E. Berry, R. T. Hemmings, B. J. Cornelius, and E. J. Anthony, "Sulphur Oxidation States in Residues From a Small-Scale Circulating Fluidized Bed Combustor" in 'Fly Ash and Coal Conversion By-Products Characterization, Utilization and Disposal V', R. T. Hemmings, E. E. Berry, G. J. McCarthy, and F. P. Glasser, Eds., Materials Res. Soc. Proc. **136**, 9 (1989).
5. L. B. Clarke, "Management of FGD Residues: An International Overview", Procd. 10th Annual Inter. Pittsburgh Coal Conf., S-H Chiang, Ed., pp 561-566 (1993).
6. D. Golden, EPRI Journal, January/February, pp 46-49 (1994).
7. C. A. Holley, Preprints, Am. Chem. Soc. Fuel Div. **36(4)**, 1761 (1991).
8. O. P. Modi, A. K. Singh, A. H. Yegneswaran, and P. K. Rohatgi, J. Materials Science lett. **11**, 1466 (1992).
9. S. Ciby, B. C. Pai, K. G. Satyanarayana, V. K. Vaidyan, and P. K. Rohatgi, J. Materials Eng Performance **2**, 353 (1993).
10. S. Jasty, P. D. Robinson, and V. M. Malhotra, Phys. Rev. B **43**, 13215 (1991).
11. R. Mu, and V. M. Malhotra, Phys. Rev. B **44**, 4296 (1991).
12. S. Jasty, and V. M. Malhotra, Phys. Rev. B **45**, 1 (1992).
13. R. C. Mackenzie and G. Berggren in 'Differential Thermal Analysis. Volume 1: Fundamental Aspects', R. C. Mackenzie, Ed., Academic Press, New York (1970).
14. O. Chaix-Plucher, J. C. Niepce, and G. Martinez, J. Materials Sci. Lett. **6**, 1231 (1987).
15. D. L. Dorsey and D. Buecker, Res. & Develop., May (1986).
16. D. N. Todor, 'Thermal Analysis of Minerals', Abacus Press, Kent (1976)

TABLE 3

This table summarizes the observed infrared bands for PCC fly ash, FBC fly ash, and FBC spent bed ash. The observed frequencies are in cm^{-1} .

PCC Fly Ash	FBC Fly Ash	FBC Spent Bed Ash	Comments	Assignment
3,642	3,642	3,642	sharp	O-H stretch $[\text{Ca}(\text{OH})_2]$
3,448	3,462	3,448	broad	O-H stretch, adsorbed water
1,631		1,624	sharp, weak	H-O-H bend of water
	1,449	1,448	broad, medium	asymmetric CO_3^{2-} stretch $[\text{CaCO}_3]$
	1144	1154	broad, strong	SO_4^{2-} stretch
	1111	1122	broad, strong	$[\text{CaSO}_4]$
1,072	1,011		broad, strong	Si-O stretch
		945	broad, weak	CaSO_3
		920	sharp, weak	O-H bend $[\text{Ca}(\text{OH})_2]$
	885		sharp, weak	CaCO_3
794	795		sharp, medium	quartz
778			sharp, weak	quartz
694			sharp, weak	quartz
	681	680	sharp, weak	Anhydrite $[\text{CaSO}_4]$
613	616	615	sharp, weak	Anhydrite $[\text{CaSO}_4]$
	602	605	sharp, weak	Anhydrite $[\text{CaSO}_4]$
593		595	sharp, weak	Anhydrite $[\text{CaSO}_4]$
560		560	broad, weak	Fe_2O_3 and Fe_3O_4
	515		broad, weak	oxides
462	462	462	broad, medium	quartz

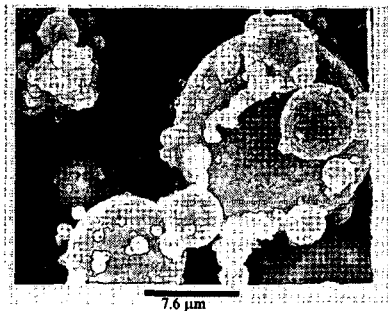


Figure 1. SEM photo of PCC fly ash showing the spherical nature of the particles.

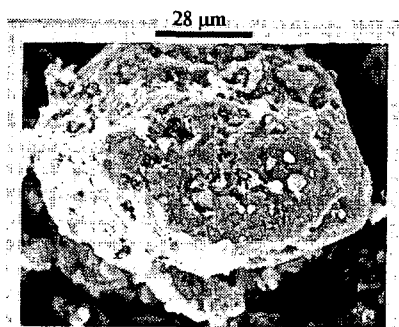


Figure 2. SEM photo of FBC fly ash.

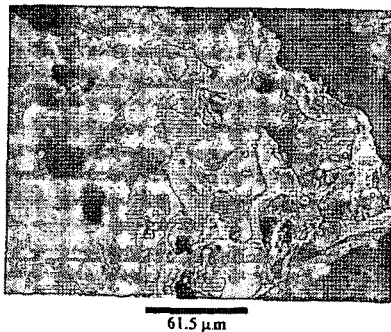


Figure 3. SEM photo of FBC spent bed ash.

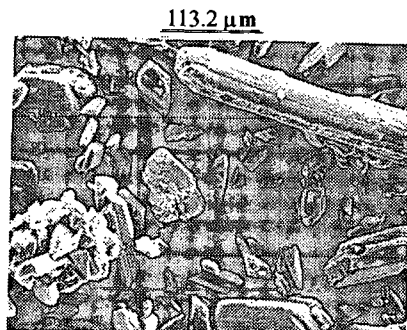


Figure 4. SEM photo of scrubber Sludge

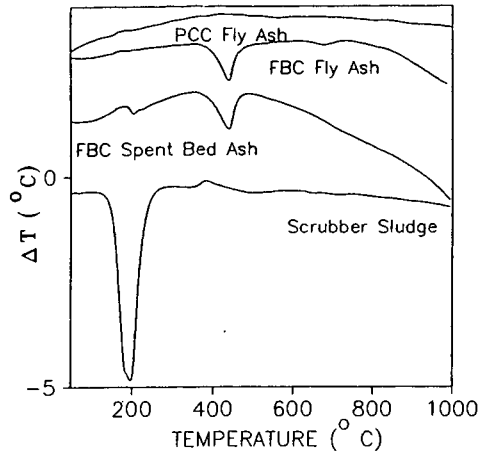


Figure 5. Differential thermal analysis (DTA) of combustion residues and scrubber sludge.

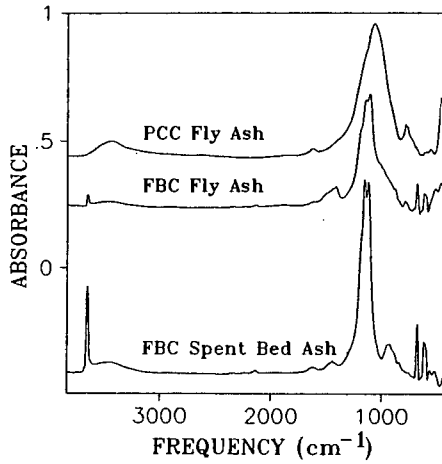


Figure 6. FTIR spectrum of combustion residues.

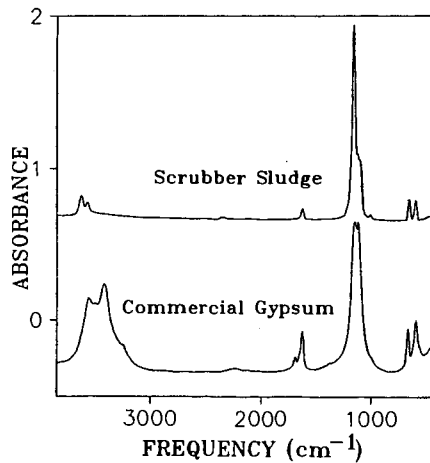


Figure 7. FTIR Spectrum of scrubber sludge and a commercial gypsum sample.